Pergamon

Int. J. Solids Structures Vol. 35, No. 20, pp. 2601–2616, 1998

0020–7683/98 $19.00 + .00

PII: S0020–7683(97)00174–1

STRENGTH OF ADHESIVELY BONDED SINGLE-LAP AND LAP-SHEAR JOINTS

L. TONG
Department of Aeronautical Engineering, University of Sydney, NSW 2006, Australia

(*Received* 29 *July* 1996; *in revised form* 3 *June* 1997)

Abstract—A simple solution procedure of predicting the strength of adhesively bonded single-lap and lap-shear unbalanced joints with nonlinear adhesive properties was developed by following the global/local analysis procedure developed by Goland and Reissner (1944). Simple formulas for the shear and peel strain energy rates of the joints were obtained in terms of the longitudinal membrane forces and the bending moments in the adherends after neglecting the terms related to the transverse shear forces. Two simple failure criteria were suggested and then validated by comparing to the measured failure envelopes and correlating with the measured strengths of the lap-shear and single-lap joints. It was shown that neglecting the terms related to the transverse shear forces could yield an over estimation of both energy rates for the single-lap joints with relatively stiff adhesive.

1. INTRODUCTION

Lap joint theories have been developed to analyse the stresses and strains in the adhesive layer for adhesively bonded lap joints (Adams and Wake, 1984; Carpenter, 1991). To predict the strength of the joints, many researchers used two types of methods, i.e., the method based on the strength of materials and the method based on fracture mechanics. In the material strength method, the maximum stresses or strains were determined using coupon tests, and then these data were used as the ultimate values of the predicted stresses or strains at a critical point or over a limited zone (Adams and Wake, 1984; Crocombe 1989; Adams, 1989, Clark and McGregor, 1993; Tong, 1994). Clark and McGregor (1993) suggested that failure occur in adhesively bonded joints when the maximum tensile stress exceeds its strength over a limited zone, and they reported that the new failure criterion is applicable to a number of joint configurations. In the fracture mechanics method, the critical energy release rate was measured and then used as the ultimate value for the predicted energy release rate or the value of J-integral (Tong, Hamaush and Ahmed, 1989; Anderson *et al.*, 1988; Chai, 1988; Fernlund *et al.*, 1994; Papini *et al.*, 1994). Fernlund *et al.* (1994) and Papini *et al.* (1994) proposed an engineering approach to predict the fracture loads for adhesive joints. In this approach the *in situ* critical energy release rate and its associated mode ratio were determined as the fracture envelope for a specific adhesive system, and then used to predict fracture loads for the bonded joints. It was shown that for the equal adherend single-lap joints, the average difference between the measured and the predicted fracture loads was 5% only. These results indicated that measurement of the *in situ* failure envelope of the adhesive system is critical in predicting joint strength.

Measurement of the *in situ* failure envelope is difficult because the complicated stresses in the adhesive need to be carefully controlled, and is also expensive due to varieties of material combinations. Hence simple and cost-effective failure criteria are always preferred. For a single-lap or lap-shear joint, the peel and shear stresses in the adhesive are considered to be predominant (Adams and Wake, 1984), and therefore it is desirable to determine an adhesive failure envelope in terms of the two stresses or the corresponding strain energy related quantities.

In this study a simple solution procedure was reported for predicting the strengths of adhesively bonded unbalanced single-lap and lap-shear joints with nonlinear adhesive properties. This procedure consists of a global/local analysis and is similar to that developed by Goland and Reissner (1944) for single-lap joints. Simple formulas for the shear and peel

strain energy rates of the joints were obtained in terms of the longitudinal membrane forces and the bending moments in both adherends after neglecting the terms related to the transverse shear forces. To predict strengths of the joints, two simple failure criteria were suggested and then validated by comparing with the measured failure envelopes of the adhesive systems and the measured strengths of the lap-shear and single-lap joints available in the literature. In addition, the effect of neglecting the terms related to the transverse shear forces was also discussed.

2. MODELING AND ASSUMPTIONS

Single-lap and lap-shear joints shown in Figs 1 and 2 are considered in this study. The adherends are modeled as cylindrically bent plates that are linearly elastic and undergo small longitudinal displacements and large lateral deflections. The adhesive is modeled as a layer capable of transmitting only peel (tensile) and shear stresses, and it is assumed that the peel and shear stress–strain behaviors can be nonlinear. Evidently, this is a nonlinear problem involving both material nonlinearity and large deformations, and it does not admit a general analytical solution for the stresses in the adhesive layer. However, similar to the case for double-lap joints (Tong, 1994), strengths of the joints can be approximately determined using simple formulas in terms of the strain energy related quantities without completely solving the nonlinear problem. To do so, we utilise the following global and local analysis procedure:

Step 1—Global analysis: in the global analysis, by neglecting the behavior of the adhesive layer and considering the large deflection only, we determine the global stress resultants in the adherends, i.e. the longitudinal membrane forces, bending moments and the transverse shear forces. For single-lap joints, these stress resultants were first given by Goland and Reissner (1944), and recently were numerically evaluated by Tsai and Morton (1994). For lap-shear joints, a similar analysis can be carried out to determine these stress resultants in the adherends. An analysis was recently presented by Lai *et al.* (1996) to study the effect of boundary conditions on the closed-form solutions for the lap-shear joints.

Step 2—Local analysis: in the local analysis, only the overlap parts in the joints will be considered. The stresses in the adhesive layer are to be determined by assuming nonlinear behavior of adhesive and using the global stress resultants in the adherends. This will be detailed in the following section.

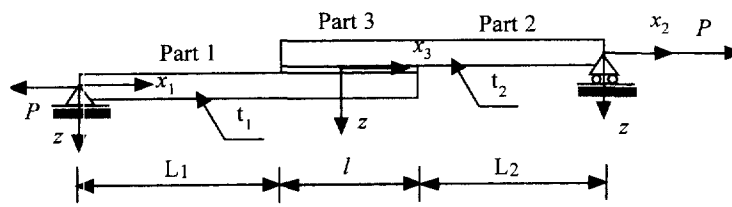

Fig. 1. Configuration for a single lap joint subjected to a tensile load.

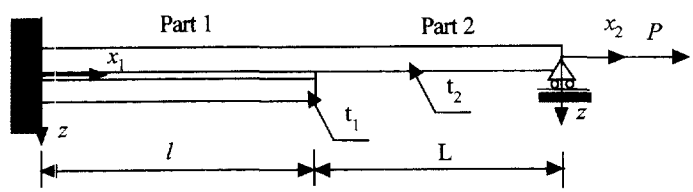

Fig. 2. Configuration for a lap shear joint subjected to a tensile load.

3. LOCAL ANALYSIS

3.1. *Governing equations*

Consider adhesive-adherend sandwiches subjected to a combination of loading at both ends as shown in Fig. 3(a) for single-lap joint and Fig. 3(b) for a lap-shear joint. The sandwich consists of two adherends and a thin adhesive layer. For an infinitesimal element shown in Fig. 4, we have the following fundamental governing equations:

For the adherend 1 and 2, the equilibrium equations are:

$$\frac{dN}{dx}+\tau=0,\quad \frac{dQ_1}{dx}+\sigma=0,\quad \frac{dM_1}{dx}-Q_1+\frac{t_1}{2}\tau=0 \tag{1a}$$

$$\frac{dN_2}{dx}-\tau=0,\quad \frac{dQ_2}{dx}-\sigma=0,\quad \frac{dM_2}{dx}-Q_2-\frac{t_2}{2}\tau=0 \tag{1b}$$

where N_i, M_i and Q_i $(i=1,2)$ are the longitudinal membrane forces, bending moments and the transverse shear forces per unit width for the two adherends, respectively.

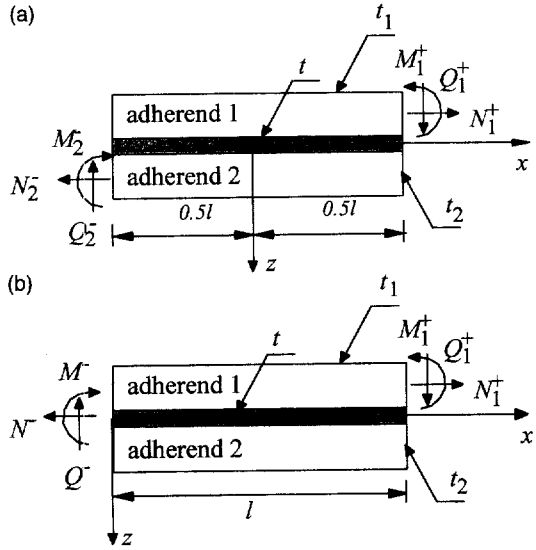

Fig. 3. (a) Stress resultants acting on both ends of an overlap in a single-lap joint. (b) Stress resultants acting on both ends of an overlap in a lap-shear joint.

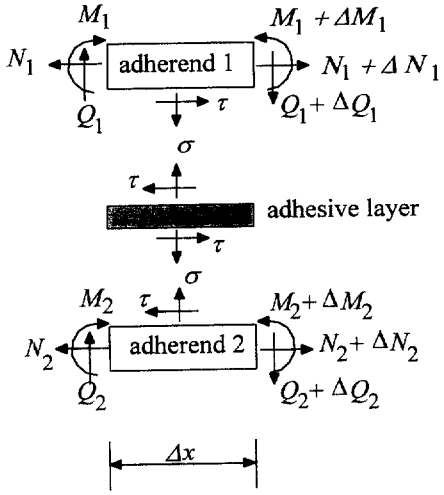

Fig. 4. Stresses and stress resultants of an infinitesimal element in the overlap.

The longitudinal membrane forces N_i $(i = 1, 2)$ and bending moments M_i $(i = 1, 2)$ for the adherend 1 and 2 can be expressed in terms of the longitudinal displacements u_i $(i = 1, 2)$ in the x direction and the lateral deflection w_i $(i = 1, 2)$ in the z direction as follows:

$$N_i = A_i \frac{du_i}{dx}, \quad M = -D_i \frac{d^2 w_i}{dx^2} \quad (i = 1, 2) \tag{2}$$

where $A_i = E_i t_i$ and $D_i = E_i t_i^3/12$ $(i = 1, 2)$ are the membrane and bending stiffness of the adherends.

In the adhesive layer, the peel stress σ and the shear stress τ are assumed to be

$$\sigma = \sigma(\varepsilon), \quad \tau = \tau(\gamma) \tag{3}$$

where $\sigma(\varepsilon)$ and $\tau(\gamma)$ are arbitrary functions of ε and γ, respectively. The shear stress–strain curve of the adhesive can be measured using either thick adherend lap shear test or napkin ring shear test, while the peel (or tensile) stress–strain curve of the adhesive can be measured using either neat adhesive tensile test or butt joint test.

The peel and shear strains in the adhesive are assumed to be constant through the adhesive thickness, and they can be defined as (Goland and Reissner, 1944; Carpenter, 1991)

$$\varepsilon = \frac{w_2 - w_1}{t}, \quad \gamma = \frac{u_2 - u_1}{t} + \frac{1}{2t}\left(t_1 \frac{dw_1}{dx} + t_2 \frac{dw_2}{dx}\right) \tag{4}$$

Equations (1)–(4) are the governing equations for the adhesive-adherend sandwich part in single-lap and lap-shear joints. Although the large deformed free adherend(s) and the sandwich part has been decoupled, eqns (1)–(4) do not admit simple solutions for the shear and peel stresses in the adhesive due to the presence of material nonlinearity in the adhesive. However, joint strength can be approximately predicted using the strain energy density method. In this method, both the shear and peel strain energy densities in adhesive are calculated without completely determining the peel and shear stresses in the adhesive.

3.2. *Bond shear strain energy rate*

Bond shear strain energy density is the area under the shear stress–strain curve for a given shear strain. Bond shear strain energy rate U_{II} is defined as the product of the adhesive thickness and the bond shear strain energy density in the adhesive. When the shear strain energy density is not constant across the adhesive layer, bond shear strain energy rate can be defined as the integration of the bond strain energy density over the adhesive thickness (Chai, 1993), or, in other words, the bond shear strain energy per unit length in the overlap direction.

To develop the expression of bond shear strain energy rate for unbalanced joints, differentiating the shear strain γ in eqn (4) with respect to x twice and using eqns (1) to (3), we find

$$\frac{d^2\gamma}{dx^2} - \frac{4}{t}\left(\frac{1}{A_2} + \frac{1}{A_1}\right)\tau(\gamma) + \frac{1}{2t}\left(\frac{t_1}{D_1}Q_1 + \frac{t_2}{D_2}Q_2\right) = 0 \tag{5}$$

Multiplying $2(d\gamma/dx)$ on both sides of the above equation, we can integrate the first term with respect to $(d\gamma/dx)^2$ and the rest with respect to γ. Using eqns (1) and (4), we can develop the following formula for the bond shear strain energy rate

$$U_{II} = t\int_0^{\gamma} \tau(\gamma)\,d\gamma$$

$$= \frac{A_1A_2}{8(A_1+A_2)}\left\{\left[\frac{N_2}{A_2} - \frac{N_1}{A_1} - \frac{t_2M_2}{2D_2} - \frac{t_1M_1}{2D_1}\right]^2 + t\left(\frac{t_1}{D_1}\int_0^{\gamma} Q_1\,d\gamma + \frac{t_2}{D_2}\int_0^{\gamma} Q_2\,d\gamma\right)\right\} \tag{6}$$

Equation (6) can be used to calculate the bond shear strain energy rate U_{II} at any point along the x axis (see Fig. 3) when the stress resultants in the two adherends are known. It is evident that the thickness and Young's modulus of both adherends can be different. In the large brackets on the right hand side of eqn (6), the first term only requires knowledge of the longitudinal membrane forces and the bending moments in both adherends, while the last two involve integration of the transverse shear forces with respect to the shear strain. It is difficult to determine the last two integrals in eqn (6) without completely solving the whole nonlinear problem. However, as an approximation, we can drop off the last two terms representing the contribution of the transverse shear forces and the shear strain in the adhesive to the bond shear strain energy rate. In doing so, an explicit and simplified linear formula for the bond shear strain energy rate can be obtained as

$$U_{II} = \frac{A_1A_2}{8(A_1+A_2)}\left[\frac{N_2}{A_2} - \frac{N_1}{A_1} - \frac{t_2M_2}{2D_2} - \frac{t_1M_1}{2D_1}\right]^2 \tag{7}$$

While it is hard to justify the effects of the neglected two terms analytically on the bond shear strain energy rate, a numerical discussion will be presented at a later stage to illustrate its effects. Global analysis of the single-lap and lap-shear joints can only determine the adherend stress resultants at the ends of the overlap. Using these stress resultants, we can approximately calculate the bond shear strain energy rate at each end of the overlap. For example, the bond shear energy rate at the right end of the overlaps in Fig. 3 can be calculated using the following equation

$$U_{II} = \frac{A_1A_2}{8(A_1+A_2)}\left(\frac{N_1^+}{A_1} + \frac{t_1M_1^+}{2D_1}\right)^2 \tag{8}$$

Equation (8) can be used to approximately calculate bond shear strain energy rate U_{II} for unbalanced single-lap and lap-shear joints using the longitudinal membrane force and the bending moment acting on one adherend that are determined in the global analysis.

3.3. *Bond peel strain energy rate*

Bond peel strain energy density is defined as the area under the peel stress–strain curve for a given peel strain. Bond peel strain energy rate U_I is defined as the product between the bond peel strain energy density and the adhesive thickness. Similar to the definition of bond shear strain energy rate, when bond peel strain energy density is not constant across the adhesive thickness, bond peel strain energy rate becomes integral of the bond peel strain energy density over the adhesive thickness.

Differentiating the peel strain ε defined in eqn (4) with respect to x four times and using eqns (1)–(3), we have

$$\frac{d^4\varepsilon}{dx^4} + \frac{1}{t}\left(\frac{t_1}{2D_1} - \frac{t_2}{2D_2}\right)\frac{d\tau(\gamma)}{dx} + \frac{1}{t}\left(\frac{1}{D_1} + \frac{1}{D_2}\right)\sigma = 0 \tag{9}$$

Multiplying $d\varepsilon/dx$ on both sides in eqn (9), integrating by part with respect to $d^3\varepsilon/dx^3$ for the first term and ε for the last two, we find

$$\frac{d^3\varepsilon}{dx^3}\frac{d\varepsilon}{dx}-\frac{1}{2}\left(\frac{d^2\varepsilon}{dx^2}\right)^2+\frac{1}{t}\left(\frac{t_1}{2D_1}-\frac{t_2}{2D_2}\right)\int_0^\tau \frac{d\varepsilon}{dx}d\tau+\frac{1}{t}\left(\frac{1}{D_1}+\frac{1}{D_2}\right)\int_0^\varepsilon \sigma\, d\varepsilon = 0$$

Evidently, the last term in the above equation is related to the bond peel strain energy rate. Now we want to express the first two terms in terms of the global transverse shear forces and bending moments. Using eqns (1), (2) and (4), we can rewrite the above equations as follows

$$\frac{2}{t}\left(\frac{1}{D_1}+\frac{1}{D_2}\right)\int_0^\varepsilon \sigma\, d\varepsilon = \frac{1}{t^2}\left(\frac{M_1}{D_1}-\frac{M_2}{D_2}\right)^2-\frac{2}{t}\left[\left(\frac{Q_1}{D_1}-\frac{Q_2}{D_2}\right)-\left(\frac{t_1}{2D_1}-\frac{t_2}{2D_2}\right)\tau\right]\frac{d\varepsilon}{dx}$$
$$-\frac{2}{t}\left(\frac{t_1}{2D_1}-\frac{t_2}{2D_2}\right)\int_0^\tau \frac{d\varepsilon}{dx}d\tau \quad (10)$$

Integration by part of the last term on the r.h.s. of eqn (10) leads to the following simplification

$$\frac{2}{t}\left(\frac{1}{D_1}+\frac{1}{D_2}\right)\int_0^\varepsilon \sigma\, d\varepsilon = \frac{1}{t^2}\left(\frac{M_2}{D_1}-\frac{M_2}{D_2}\right)^2-\frac{2}{t}\left(\frac{Q_1}{D_1}-\frac{Q_2}{D_2}\right)\frac{d\varepsilon}{dx}$$
$$+\frac{2}{t}\left(\frac{t_1}{2D_1}-\frac{t_2}{2D_2}\right)\int_0^{d\varepsilon/dx}\tau\, d\left(\frac{d\varepsilon}{dx}\right) \quad (11)$$

It is noted that the last term on the r.h.s. of eqn (11) represents the contribution to the bond peel strain energy when the stiffness of both adherends are different. By expressing the shear stress τ in terms of the shear forces and bending moments using the third equation in eqns (1a) and (1b), we have

$$\frac{t_1+t_2}{2}\tau = Q_1+Q_2-\left(\frac{dM_1}{dx}+\frac{dM_2}{dx}\right)$$

Using the first equation in eqns (4) and noting that Q_1+Q_2 is constant, we finally rewrite eqn (11) as follows

$$U_1 = t\int_0^{\varepsilon_0}\sigma(\varepsilon)\, d\varepsilon$$
$$=\frac{D_1D_2}{2(D_1+D_2)}\left(\frac{M_1}{D_1}-\frac{M_2}{D_2}\right)^2-\frac{D_1D_2t}{(D_1+D_2)}\left(\frac{Q_1}{D_1}-\frac{Q_2}{D_2}\right)\frac{d\varepsilon}{dx}$$
$$+\frac{(t_1D_2-t_2D_1)t}{(D_1+D_2)(t_1+t_2)}(Q_1+Q_2)\frac{d\varepsilon}{dx}$$
$$-\frac{(t_1D_2-t_2D_1)}{2(D_1+D_2)(t_1+t_2)}\left[\frac{M_1^2}{D_1}+2\left(\frac{1}{D_1}-\frac{1}{D_2}\right)M_1M_2-\frac{M_2^2}{D_2}\right]$$
$$+\frac{(t_1D_2-t_2D_1)}{(D_1+D_2)(t_1+t_2)}\left(\frac{1}{D_2}\int_0^{M_1}M_2\, dM_1+\frac{1}{D_1}\int_0^{M_2}M_1\, dM_2\right) \quad (12)$$

Evidently, longitudinal membrane forces in both adherends do not contribute to the bond peel strain energy rate. Equation (12) is an accurate expression of the bond peel strain energy rate in terms of the bending moments, transverse shear forces in both adherends as well as the slope of the peel strain distribution for an unbalanced lap joints. However,

presence of the term $d\varepsilon/dx$ indicates coupling between the global and local analysis. By dropping off the terms related to $d\varepsilon/dx$, we have the following approximate expression for the bond peel strain energy rate

$$U_I = \frac{D_1 D_2}{2(D_1+D_2)}\left(\frac{M_1}{D_1}-\frac{M_2}{D_1}\right)^2 - \frac{(t_1 D_2 - t_2 D_1)}{2(D_1+D_2)(t_1+t_2)}\left[\frac{M_1^2}{D_1}+2\left(\frac{1}{D_1}-\frac{1}{D_2}\right)M_1 M_2 - \frac{M_2^2}{D_2}\right] + \frac{(t_1 D_2 - t_2 D_1)}{(D_1+D_2)(t_1+t_2)}\left(\frac{1}{D_1}\int_0^{M_1} M_2\, dM_1 - \frac{1}{D_1}\int_0^{M_2} M_1\, dM_2\right) \quad (13)$$

Equation (13) reveals that bond peel strain energy rate can be approximately determined in terms of the bending moments in both adherends. For a DCB (Double Cantilever Beam) specimen, eqn (13) is accurate. For a single-lap joint, it was assumed $(dw_1/dx) = (dw_2/dx)$ (see Hart-Smith, 1973; Oplinger, 1991; Tsai and Morton, 1994) and this assumption implies an approximation of $(d\varepsilon/dx) = 0$. For single-lap and lap-shear joints, at the end of the overlap, see for example at the right end, eqn (13) becomes

$$U_I = \frac{D_2}{2(D_1+D_2)D_1}(M_1^+)^2 - \frac{(t_1 D_2 - t_2 D_1)}{2(D_1+D_2)(t_1+t_2)}\frac{(M_1^+)^2}{D_1} \quad (14)$$

Equation (14) unveils that bond peel strain energy rate at the right end of the single-lap and lap-shear joints can be determined using the bending moment acting on adherend 1.

It is worth pointing out that although the basic eqns (5) and (9) are nonlinear, the final formulas for both bond shear and peel strain energy rates are linear due to the assumptions of neglecting the contributions of the transverse shear forces to the bond strain energy rates.

3.4. *Bond strain energy rate*

Bond strain energy density is defined as the sum of the area under the shear stress–strain curve for a given shear strain and the area under the peel stress–strain curve for a given peel strain. Similarly, bond strain energy rate is defined as the product of adhesive thickness and the bond strain energy density. For more general case, it can be defined as the integration of the bond strain energy density over the adhesive thickness. For a given shear and peel strain, bond strain energy rate is given by

$$U(\psi) = U_{II} + U_I \quad (15)$$

where ψ is the strain energy ratio defined by

$$\psi = \arctan\left(\sqrt{\frac{U_{II}}{U_I}}\right) \quad (16)$$

where U_I and U_{II} are the bond peel and shear strain energy rates, respectively. The strain energy ratio is 0° when adhesive is subjected to pure peel strain and 90° when subjected to pure shear strain, and varies from 0–90° when subjected to combined shear and peel strains.

For single-lap and shear lap joints subjected to a given load P as shown in Figs 1 and 2, the bond strain energy rate at the ends of the overlap can be computed using eqn (10) and eqns (14)–(16) in terms of the membrane forces and the bending moments. When an appropriate failure criterion is used, the failure load or strength for the joints can then be determined.

4. FAILURE CRITERIA AND STRENGTH PREDICTION

A failure criterion can be postulated as: bond or adhesive failure in adhesively-bonded lap joints occurs when the maximum bond strain energy rate in the adhesive layer attains its ultimate value U_C for a combined shear and peel strain or a strain energy ratio, namely,

$$U(\psi) = U_C(\psi) \tag{17}$$

Where $U_C(\psi)$ is the adhesive failure envelope that is defined as the critical strain energy rate of the adhesive corresponding to various combinations of shear and peel strains. It is desirable to measure the whole *in situ* failure envelope for a specific material combination. However, measurement of such *in situ* failure envelope requires enormous effort and is only applicable to the particular material combination, thus can be very expensive. For this reason, we will use the following interactive failure criterion:

$$\left(\frac{U_{II}}{U_{IIC}}\right)^{\alpha} + \left(\frac{U_I}{U_{IC}}\right)^{\beta} = 1 \tag{18}$$

where α and β are real constants, and U_{IC} and U_{IIC} are the critical bond strain energy rates of pure peel and pure shear, respectively. In the following section, we will evaluate the following two simple ones:

Linear failure criterion ($\alpha = \beta = 1$):

$$\frac{U_{II}}{U_{IIC}} + \frac{U_I}{U_{IC}} = 1 \tag{19}$$

Quadratic failure criterion ($\alpha = \beta = 2$):

$$\left(\frac{U_{II}}{U_{IIC}}\right)^2 + \left(\frac{U_I}{U_{IC}}\right)^2 = 1 \tag{20}$$

The failure criteria presented above are similar in form to the fracture criterion for bonded joints presented by Chai (1988).

5. NUMERICAL RESULTS AND DISCUSSIONS

5.1. *Comparison of failure envelopes*

For a balanced single-lap joint, Tong (1996) showed that the bond shear and bond peel strain energy rates are equivalent to the Mode II and I energy release rates, respectively, and bond strain energy rate equals to the mixed mode energy release rate. It was also demonstrated that the strain energy rate ratio is identical to the mode ratio of the mixed mode I and mode II fracture. It was concluded that there exists a equivalence between the fracture envelope $J_c(\psi)$ (measured by Fernlund *et al.* (1994) and Papini *et al.* (1994)) and the bond failure envelope $U_C(\psi)$. Hence these fracture envelopes will be used as the bond failure envelopes to assess the two simple failure criteria. To do this, the failure envelopes developed using the two failure criteria as given in eqns (19) and (20) are compared to the measured *in situ* failure envelopes $U_C(\psi)$ available in the literature.

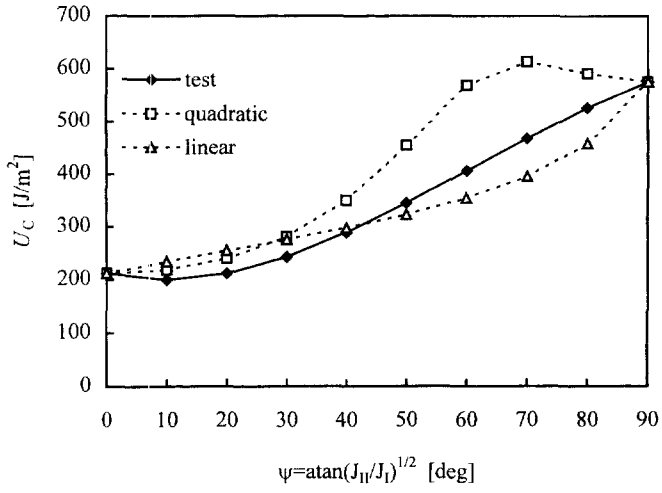

Fig. 5. Failure envelopes, U_c vs phase angle ψ, for 7075-T6 aluminum adherends bonded with Cybond 4523GB epoxy adhesive system (test curve taken from Fernlund *et al.*, 1994).

Figure 5 depicts the values of U_C computed using eqns (19) and (20) with $U_{IC} = 212$ J/m^2 and $U_{IIC} = 575$ J/m^2 vs the phase angle. The present calculated failure envelopes are also compared with the *in situ* mixed failure envelope measured by Fernlund *et al.* (1994). It is shown that U_C given by the quadratic is always larger than the measured, and U_C computed using the linear criterion is larger than the measured when the phase angle is less than about 43°, and is less than the measured when the phase angle is larger than 43°. For the linear criterion, the relative deviations are between −20 and 25%, while for the quadratic criterion, the relative difference can be as high as 40%. It is also revealed that the linear criterion tends to be more appropriate when the phase angle is larger than 34°. It is noted that the quadratic criterion over predict U_C and thus, can result in an unconservative failure prediction.

Figure 6 plots the bond strain energy rate U_C computed using eqns (19) and (20) with $U_{IC} = 794$ J/m^2 and $U_{IIC} = 5605$ J/m^2 vs the phase angle. The *in situ* mixed type failure envelope measured by Papini *et al.* (1994) is also plotted in Fig. 6 for comparison. It is noted that bond strain energy rate U_C predicted by the quadratic criterion in eqn (20) is not larger than the measured when the phase angle is less than 58°, and is larger than the measured when the phase angle is larger than 58°. The value of U_C computed using the

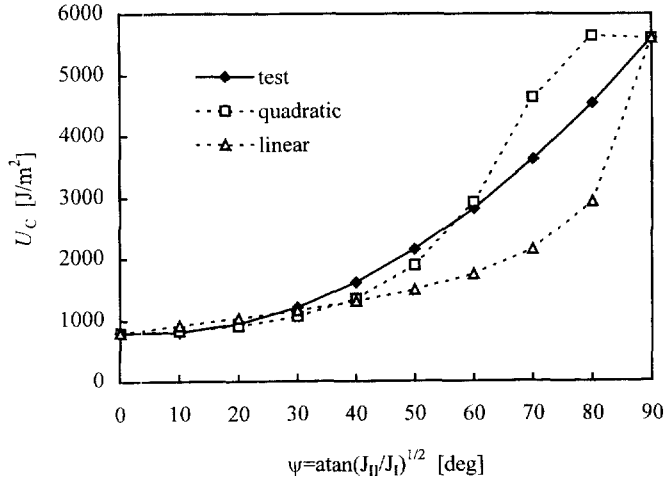

Fig. 6. Failure envelopes, U_c vs phase angle ψ, for 7075-T6 aluminum adherends bonded with Permabond ESP 310 adhesive system (test curve taken from Papini *et al.*, 1994).

linear criterion is larger than the measured when the phase angle is less than about 27°, and is less than the measured when the phase angle is larger than 27°. In this case, there is little difference between the quadratic and the linear criterion when the phase angle is less than 40°. When the phase angle is greater than 40°, the quadratic criterion tends to be more appropriate than the linear criterion as it is more close to the measured curve.

It is noted that the present two simple failure criteria given in eqns (19) and (20) can be used to generate approximate failure envelopes. In this case, only the critical values of bond strain energy rate subjected to pure peel and shear need to be measured.

5.2. *Comparison of strength for lap-shear and single-lap joints*

For a given single-lap or lap-shear joint subjected to a given load as shown in Fig. 1 or Fig. 2, we can determine the longitudinal membrane forces and the bending moments at the ends of the overlap and then calculate the shear and peel strain energy rates. By using the failure criteria given by eqns (19) and (20) and the measured *in situ* envelopes (Fernlund *et al.*; 1994; Papini *et al.*, 1994), we can determine the strength of the joint after following an iterative numerical procedure. The predicted strengths are then compared with the measured ones available in the literature.

Table 1 gives the fracture loads for the lap-shear joints predicted using the present two failure criteria and compares with the measured fracture loads taken from Fernlund *et al.* (1994). Between the two criteria, the linear criterion tends to give the smallest average difference 5.6%, while the quadratic criterion yields an average difference of 17.1%. Evidently, linear criterion is appropriate for predicting the strength for the lap shear joints. This is because the linear criterion fits best to the measured failure envelope in Fig. 5 when the theoretical phase angle varies from 49.1–90° for pinned equal adherend lap shear joints (Papini *et al.*, 1994).

Table 2 compares the fracture loads predicted using the present two failure criteria and the measured fracture loads for the single-lap joints made of the 7075-T6 aluminum adherends bonded with Cybond 4523GB epoxy adhesive system (Fernlund *et al.*, 1994). It is noted that the quadratic criterion gives the average difference of 11.9%, and the linear yields an average difference of 5.9%. It is thus found that the linear criterion seems to be the appropriate one for these joints.

In Table 3, the measured and predicted fracture loads are tabulated for the single-lap joints made of the 7075-T6 aluminum adherends bonded with Permabond ESP 310 adhesive

Table 1. Comparison of predicted and measured fracture loads (N/mm) for equal adherend lap shear joints ($t_1 = t_2 = 12.54$ mm, width was 20 mm)

Geometry (mm)		Measured and predicted fracture load using various types of criteria [see eqns (19) and (20)]			
L	l	Test*	*In situ*†	Linear	Quadratic
160	187	1100	971 (−117)	965 (−12.3)	1174 (6.7)
165	185	968	962 (−0.6)	955 (−1.3)	1164 (20.3)
187	159	876	883 (0.8)	876 (0.0)	1071 (22.3)
182	154	915	874 (−4.5)	866 (−5.4)	1059 (15.7)
162	180	935	953 (1.9)	947 (1.3)	1153 (23.3)
143	197	1092	1013 (−7.2)	1008 (−7.7)	1221 (11.8)
213	127	726	786 (8.3)	777 (7.0)	951 (31.0)
154	192	1044	988 (−5.4)	982 (−5.9)	1194 (14.4)
143	196	1081	1011 (−6.5)	1006 (−6.9)	1218 (12.7)
220	118	769	758 (−1.4)	750 (−2.5)	916 (19.1)
133	210	1226	1055 (−13.9)	1050 (−14.4)	1267 (3.3)
187	157	966	878 (−9.1)	871 (−9.8)	1065 (10.2)
242	101	720	703 (−2.4)	695 (−3.5)	846 (17.5)
168	184	960	957 (−0.3)	950 (−1.0)	1158 (20.6)
240	112	695	735 (5.8)	727 (4.6)	888 (27.8)
Average difference E (%)			(5.3)	(5.6)	(17.1)

* Data taken from Pernlund *et al.* (1994).

† Results obtained using failure envelopes given by Pernlund *et al.* (1994).

Table 2. Comparison of predicted and measured fracture load (N/mm) for equal adherend single lap joints ($t_1 = t_2 = 12.5$ mm, width was 20 mm)

Geometry (mm)			Measured and predicted fracture load using various types of criteria [see eqns (19) and (20)]			
L_1	l	L_2	Test*	*In situ*†	Linear	Quadratic
141	86	125	572	533 (−3.3)	546 (−4.5)	646 (12.9)
144	82	125	555	545 (−1.8)	539 (−2.9)	638 (14.9)
178	82	141	547	522 (−4.6)	515 (−5.8)	610 (11.5)
176	86	138	525	527 (0.4)	521 (−0.8)	618 (17.7)
245	75	80	438	419 (−4.3)	414 (−5.5)	492 (12.3)
265	55	80	391	385 (−1.5)	380 (−2.8)	449 (14.8)
216	98	88	497	475 (−4.4)	469 (−5.6)	561 (12.9)
203	62	135	551	470 (−14.7)	464 (−15.8)	549 (−0.4)
185	109	97	544	521 (−4.2)	514 (−5.5)	615 (13.0)
219	74	96	469	445 (−5.1)	439 (−6.4)	522 (11.3)
167	127	96	565	565 (0.0)	558 (−1.2)	670 (18.6)
134	56	108	530	491 (−7.4)	485 (−8.5)	570 (7.5)
202	105	57	496	453 (−8.7)	447 (−9.9)	533 (7.5)
196	111	94	559	514 (−8.1)	507 (−9.3)	607 (8.6)
216	92	82	525	458 (−12.8)	452 (−13.9)	540 (2.9)
148	115	106	574	576 (0.3)	569 (−0.9)	679 (18.3)
148	115	106	595	576 (−3.2)	569 (−4.4)	679 (14.1)
148	115	106	587	576 (−1.9)	569 (−3.1)	679 (15.7)
Average difference E (%)				(4.8)	(5.9)	(11.9)

* Data taken from Pernlund *et al.* (1994).
† Results obtained using failure envelopes given by Pernlund *et al.* (1994).

Table 3. Comparison of measured and predicted fracture loads (N/mm) for equal-adherend single lap joints ($t_1 = t_2 = 12.7$ mm)

Geometry (mm)			Measured and predicted fracture loads using various types of criteria [see eqns (19) and (20)]			
L_1	l	L_2	Test*	*In situ*†	Linear	Quadratic
142	80	140	1408	1514 (7.5)	1289 (−8.5)	1429 (1.5)
142	80	140	1352	1514 (12.0)	1289 (−4.7)	1429 (5.7)
142	80	140	1361	1514 (11.2)	1289 (−5.3)	1429 (5.0)
142	80	140	1405	1514 (7.8)	1289 (−8.3)	1429 (1.7)
142	80	140	1450	1514 (4.4)	1289 (−11.1)	1429 (−1.4)
227	81	148	1478	1452 (−1.8)	1222 (−17.3)	1361 (−7.9)
227	81	148	1481	1452 (−2.0)	1222 (−17.5)	1361 (−8.1)
227	81	148	1524	1452 (−4.7)	1222 (−19.8)	1361 (−10.7)
254	54	148	1379	1284 (−6.9)	1083 (−21.5)	1195 (−13.3)
249	59	148	1373	1315 (−4.2)	1108 (−19.3)	1225 (−10.8)
227	64	171	1284	1367 (6.5)	1157 (−9.9)	1279 (−0.4)
172	117	172	1654	1721 (4.1)	1458 (−11.9)	1638 (−1.0)
200	90	171	1477	1534 (3.9)	1297 (−12.2)	1445 (−2.2)
237	53	171	1308	1301 (−0.5)	1102 (−15.7)	1214 (−7.2)
197	82	192	1493	1496 (0.2)	1268 (−15.1)	1408 (−5.7)
166	140	165	1768	1867 (5.6)	1581 (−10.6)	1791 (1.3)
203	104	164	1647	1615 (−1.9)	1362 (−17.3)	1526 (−7.3)
230	80	164	1457	1457 (0.0)	1229 (−15.6)	1367 (−6.2)
Average difference E (%)				(4.7)	(13.4)	(5.4)

* Data taken from Papini *et al.* (1994).
† Results obtained using failure envelopes given by Papini *et al.* (1994).

system (Papini *et al.*, 1994). It is shown that the linear criterion gives an average difference of 13.4%, while the quadratic results in an average differences of 5.4% for these joints. Clearly the quadratic criterion seems to be appropriate for predicting the strengths of the joints manufactured using the adhesive system.

6. EFFECT OF TRANSVERSE SHEAR FORCE

In the above sections, we neglected the terms related to the transverse shear forces when deriving the simple formulas for the bond shear and peel strain energy rates. However, it was not clear to what extent the terms related to the transverse shear forces affect the prediction of these strain energy rates. In this section, a numerical evaluation will be given for adhesively bonded single-lap joints subjected to axially applied load. For simplicity, we consider the case of linear elastic adhesive behavior. In this case, the Goland and Reissner's solutions (1944) for both shear and peel stresses can be employed to calculate the strain energy rates and then used together with the finite element analysis (FEA) to benchmark the effect of these neglected terms related to the transverse shear forces.

Let us consider adhesively bonded balanced single-lap joints subjected to applied tensile force P as shown in Fig. 1. The free lengths of the joints are assumed to be $L_1 = L_2 = 100$ mm. The overlap length is taken as $l = 80$ mm. Both adherends have the same thickness of $t_1 = t_2 = 1$ mm. The thickness of adhesive layer is $t = 0.2$ mm. We assume that the adhesive exhibits a linear elastic behavior with Young's modulus of $E = 2.150$ GPa and Poisson ratio of $v = 0.34$. The two adherends have the same Young's modulus of $E_1 = E_2 = 70$ GPa and Poisson ratio of $v_1 = v_2 = 0.3$. Before presenting the results, let us introduce the following parameter used by Goland and Reissner (1944)

$$\beta = \sqrt{\frac{8Gt_1}{E_1 t}} \tag{21}$$

where G is the shear modulus of the adhesive. To study the effect of this parameter β, the

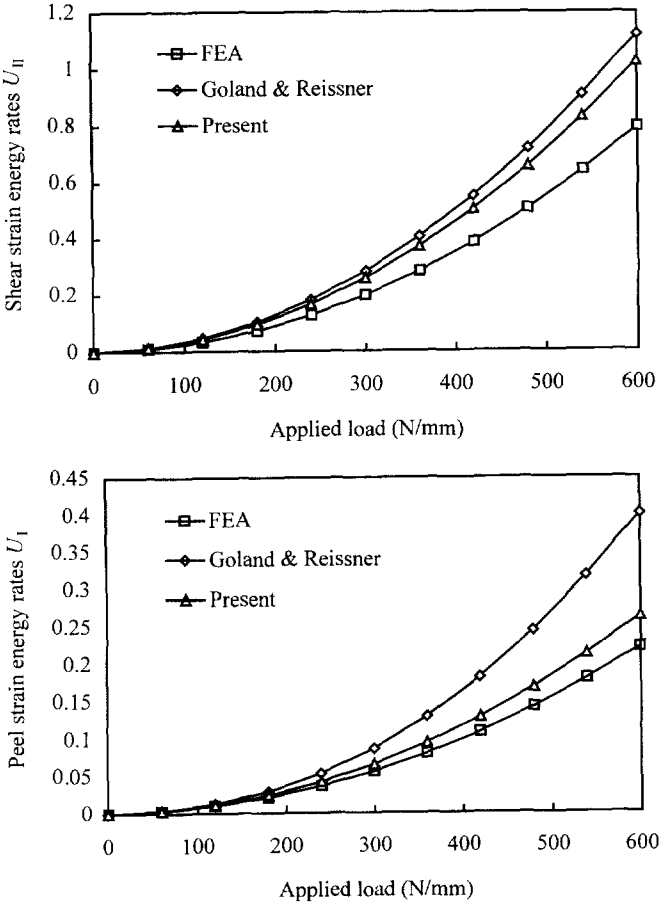

Fig. 7. (a) Shear strain energy U_{II} vs applied load for single-lap joints with $\beta l/2t = 27.1$. (b) Peel strain energy U_I vs applied load for single-lap joints with $\beta l/2t = 27.1$.

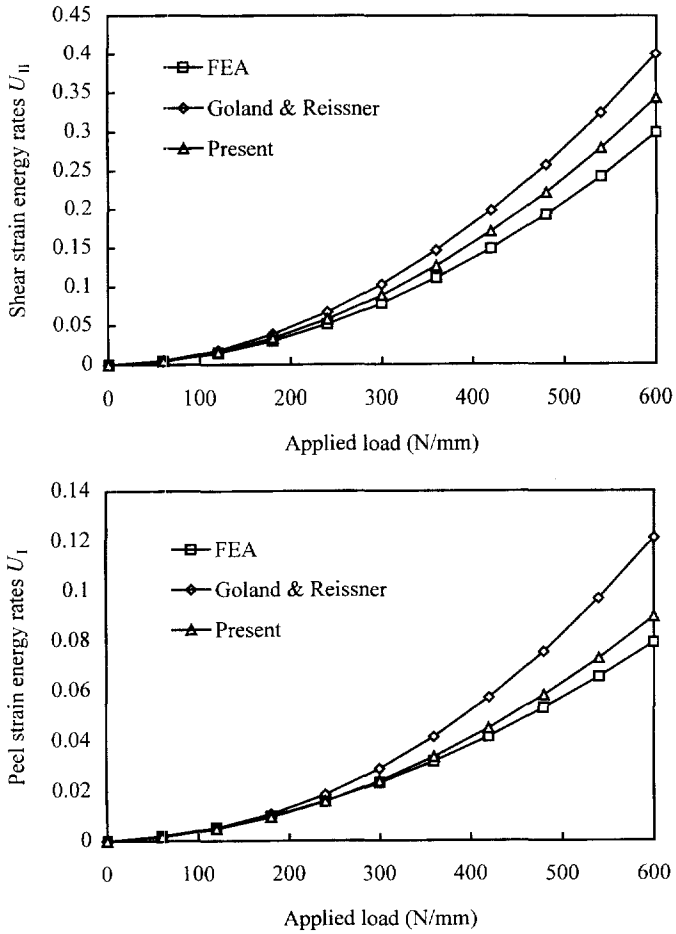

Fig. 8. (a) Shear strain energy U_{II} vs applied load for single-lap joints with $\beta l/2t = 15.6$. (b) Peel strain energy U_I vs applied load for single-lap joints with $\beta l/2t = 15.6$.

Young's modulus of the adherends is varied from 70–420 GPa in all calculations. Obviously, as the Young's modulus of the adherends increases, the value of parameter β decreases, and thus the adhesive layer becomes mor flexible relative to the adherends.

In the calculations, the general expressions for the shear and peel stresses developed by Goland and Reissner (1944) are used to calculate the shear and peel strain energy rates, respectively. The present results are computed using eqns (8) and (14), and the longitudinal membrane forces and the bending moments determined via the global analysis of the joints. In the finite element analysis, 2-D plane strain models including large deflections are established using 4-node quadrilateral elements in the Strand 6 (G+D, 1993). In the first meshing scheme, in the vicinities of the overlap ends, one element in the thickness direction is used to model the adhesive layer and four elements are utilised in the thickness direction to model each adherend. In the second meshing scheme, two elements across the adhesive thickness near the end of the adhesive layer were used (Tsai and Morton, 1994). However, there was a very small difference noted between the two schemes. Thus in the following discussion, we only report the results obtained using the first meshing scheme.

Figures 7 and 8 depict the plots of the shear and peel strain energy rates vs the applied load for the single-lap joints with $\beta l/2t = 27.1$ and 15.6, respectively. It is clearly shown that the present results for both strain energy rates are less than those predicted using the Goland and Reissner's solution and larger than the FEA results. The differences between the present results and the other two predictions are very small when the applied load is low and becomes large when the applied load is increased. As the load is increased, the

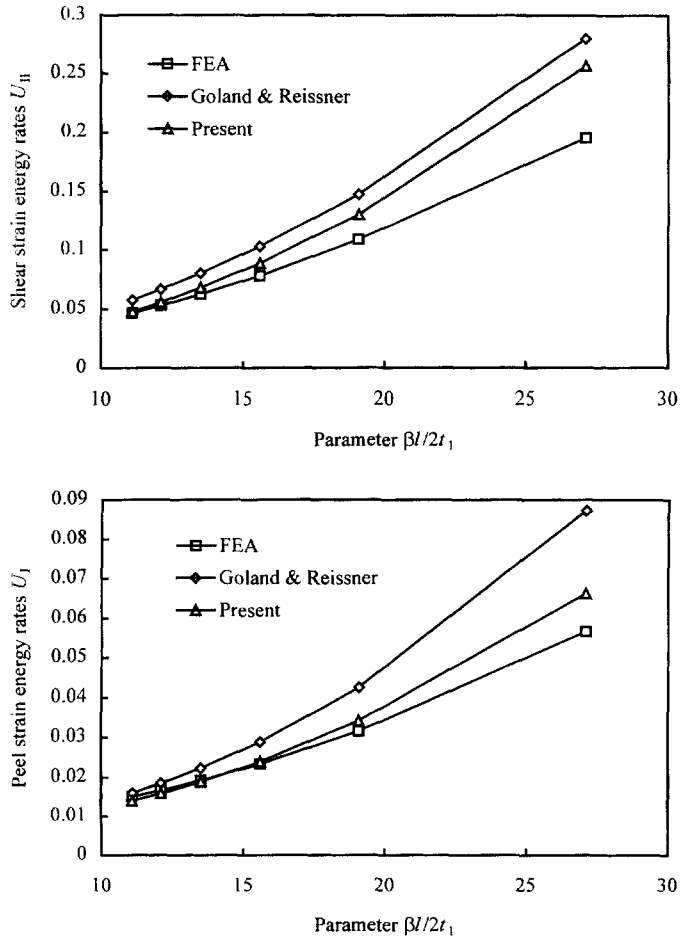

Fig. 9. (a) Shear strain energy U_{II} vs parameter $\beta l/2t$ for single-lap joints subjected to the applied load of $P = 300$ N. (b) Peel strain energy U_I vs parameter $\beta l/2t$ for single-lap joints subjected to the applied load of $P = 300$ N.

present results of the peel strain energy rate are close to the FEA results for both $\beta = l/2t = 27.1$ and 15.6, whereas, the present results for the shear strain energy rate are close to the Goland and Reissner's results when $\beta l/2t = 27.1$. The effect of parameter $\beta l/2t$ on both strain energy rates is shown in Figs 9 and 10 for the single-lap joints subjected to the applied load of $P = 300$ N and 600 N, respectively. It is noted that both strain energy rates increase with the parameter $\beta l/2t$, and the present results are less than those calculated using the Goland and Reissner's solutions and are larger than the FEA results for almost all values of $\beta l/2t$. When comparing with the FEA results, the present results tend to be better than those computed using the Goland and Reissner solutions for both peel and shear strain energy rates. When parameter $\beta l/2t$ is small, namely, for these joints with relative flexible adhesive, there is a good agreement between present results and the FEA ones; when parameter $\beta l/2t$ is large, e.g., for the joints with relatively stiff adhesive, the present results for both strain energy rates tend to be larger than the FEA ones, and the deviation becomes large as the applied load is increased. Thus, when neglecting the terms related to the transverse shear forces, the shear and peel strain energy rates can be predicted reasonably well using eqns (10) and (14) for the joints with relatively flexible adhesive. From these results, it is noted that the terms related to the transverse shear forces has a slight effect on the predictions of the shear and peel strain energy rates for the joints with relatively flexible adhesive, and has a noticeable effect on the calculations of both strain energy rates when the adhesive is relatively stiff.

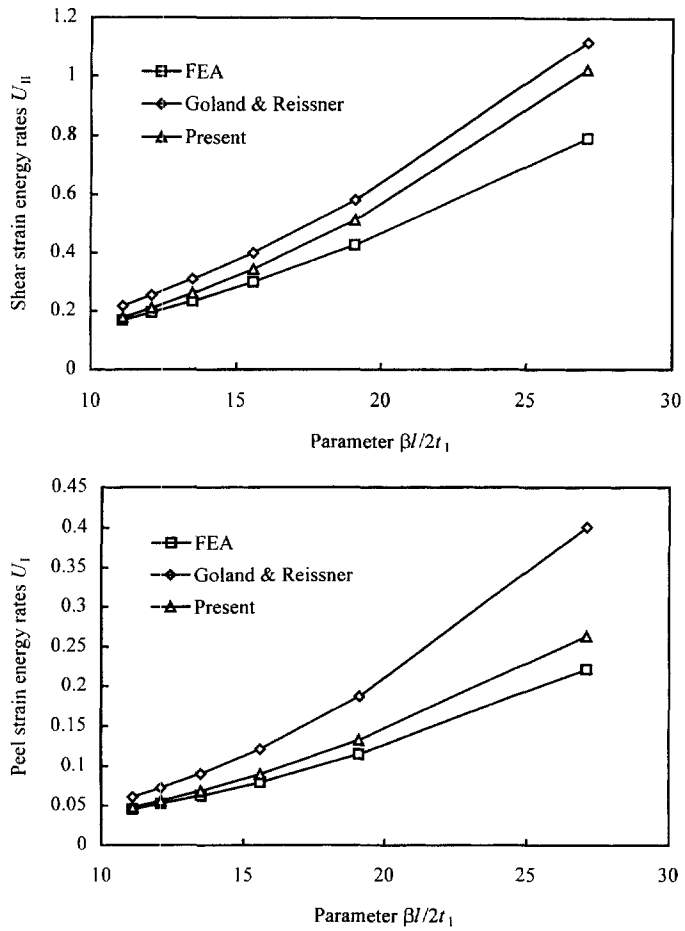

Fig. 10. (a) Shear strain energy U_{II} vs parameter $\beta l/2t$ for single-lap joints subjected to the applied load of $P = 600$ N. (b) Peel strain energy U_I vs parameter $\beta l/2t$ for single-lap joints subjected to the applied load of $P = 600$ N.

7. CONCLUSIONS

This paper presented a simple solution procedure for predicting the strengths of adhesively bonded single-lap and lap-shear joints with nonlinear adhesive properties. Following a global/local analysis procedure, simple formulas were developed for the shear and peel strain energy rates in the adhesively bonded joints with unbalanced adherends. The shear and peel strain energy rates were expressed in terms of the longitudinal membrane forces and the bending moments in the adherends after neglecting the terms related to the transverse shear forces. Two simple failure criteria were suggested and then evaluated by comparing to the measured *in situ* failure envelopes and the measured strengths of the lap-shear and single-lap joints. It was shown that neglecting the terms related to the transverse shear forces has a slight effect on predictions of both strain energy rates when the adhesive is relatively flexible, and tends to yield a noticeable effect on both strain energy rates when the adhesive is relatively stiff.

REFERENCES

Adams, R. D. and Wake, W. C. (1984) *Structural Adhesive Joints in Engineering*. Elsevier Applied Science Publishers, London.

Adams, R. D. (1989) Strength predictions for lap joints, especially with composite adherends. A review. *Journal of Adhesion* **30**, 219–242.

Anderson, G. P., Brinton, S. H., Ninow, K. J. and DeVries, K. L. (1988) A fracture mechanics approach to predicting bond strength. In *Advances in Adhesively Bonded Joints*, pp. 93–101. ASME, New York.

Carpenter, W. C. (1991) A comparison of numerous lap joint theories for adhesively bonded joints. *Journal of Adhesion* **35,** 55–73.
Chai, H. (1988) Shear fracture. *International Journal of Fracture* **37,** 137–159.
Chai, H. (1993) Observation of deformation and damage at the tip of cracks in adhesive bonds loaded in shear and assessment of a criterion for fracture. *International Journal of Fracture* **60,** 311–326.
Clark, J. D. and McGregor, I. J. (1993) Ultimate tensile stress over a zone: a new failure criterion for adhesive joints, *Journal of Adhesion* **52,** 227–245.
Crocombe, A. D. (1989) Global yielding as a failure criteria for bonded joints. *International Journal of Adhesion and Adhesives* **9**(3), 145–153.
Fernlund, G., Papini, M., McCammond, D. and Spelt, J. K. (1994) Fracture load predictions for adhesive joints. *Composite Science and Technology* **51,** 587–600.
G+D Computing (1993) Strand6—finite element analysis system. Sydney, Australia.
Goland, M. and Reissner, E. (1944) The stresses in cemented joints. *ASME Journal of Applied Mechanics* **11,** A17–A27.
Hamaush, S. A. and Ahmed, S. H. (1989) Fracture energy release rate of adhesive joints. *International Journal of Adhesion and Adhesives* **9,** 171–178.
Hart-Smith, L. J. (1973) Adhesive-bonded single lap joints. Langley Research Center, NASA Cr-112236, Hampton, Virginia.
Lai, Y.-H., Rakestraw, M. D. and Dillard, D. A. (1996) The cracked lap shear specimen revisited—a closed form solution. *International Journal of Solids and Structures* **33,** 1725–1743.
Oplinger, D. W. (1991) A layered beam theory for single lap joints. Army Materials Technology Laboratory Report MTL TR91-23.
Papini, G., Fernlund, G. and Spelt, J. K. (1994) The effect of geometry on the fracture of adhesive joints. *International Journal of Adhesion and Adhesives* **14,** 5–13.
Tong, L. (1994) Bond shear strength for adhesive bonded double lap joints. *International Journal of Solids and Structures* **31,** 2919–2931.
Tong, L. (1996) Bond strength for adhesive bonded single lap joints. *Acta Mechanica* **117,** 101–113.
Tsai, M. Y. and Morton, J. (1994) An evaluation of analytical and numerical solutions to the single-lap joints. *International Journal of Solids and Structures* **31,** 2537–2563.